CLM-P753

CLM-P753

UKAEA

Preprint

A MULTICHANNEL SPECTROMETER FOR PLASMA DIAGNOSTICS

P G CAROLAN
A PATEL

CULHAM LABORATORY
Abingdon Oxfordshire
1985

CLM-P753

A MULTICHANNEL SPECTROMETER FOR PLASMA DIAGNOSTICS

P G Carolan and A Patel*

Culham Laboratory, Abingdon, Oxon OX14 3DB, UK

(UKAEA/Euratom Fusion Association)

Abstract

A multichannel vacuum ultraviolet spectrometer has been constructed to provide time-resolved measurements of line radiation from a plasma. The spectrometer may simultaneously view up to 40 pre-selected narrow spectral bands or lines from a common viewing chord in a wide spectral region (~60-450 nm) with the maximum frequency response limited to 80 MHz by the photomultipliers and 350 kHz by the data acquisition system. Rapid reselection of impurity lines is facilitated by the use of multiple slits cut in a metal foil placed at the Rowland circle of the instrument. Due to the limitation imposed by the present fibre optic coupling to the plasma the results to date are from impurity wavelength in excess of about 220 nm.

(Submitted for publication in Review of Scientific Instruments)

* Royal Holloway College (University of London)

June 1985

Introduction

Impurities play an important role in determining the characteristics of most toroidal plasma systems. Through radiation, resistivity, thermal conduction and charge exchange, they may influence the confinement of such systems. Impurities such as Oxygen, Carbon, Chromium, Molybdenum and Iron (which may be constituents of the vacuum vessel) may enter the plasma by mechanisms such as desorption, eg Oxygen from the walls, so the study of these impurities and production mechanisms are of great value. Stripping of electrons from the impurities and the subsequent line emission is dependent on local plasma electron temperatures and densities. The monitoring of line radiation corresponding to different ionization states can yield information on local ion abundances and impurity influx and transport for given electron temperature and density profiles. For example, in the HBTX1A Reversed Field Pinch [1] at axial plasma temperatures of ~ 100 eV, CII is abundant in the plasma periphery, whilst the CV population is in the broad central plasma region [2]. Also, the influx rates of various impurities depend on plasma-wall interaction, for example from sputtering [3], which is strongly dependent on plasma edge temperatures, local plasma movements and instabilities.

In plasmas of thermonuclear interest, resonance emission lines from highly ionised impurities are generally observed in the VUV (60-200 nm) and XUV regions (< 60 nm), and due to the importance of plasma-wall phenomena [3], low ionization or neutral impurity lines are also of interest (UV-visible region). Hence there is a need for a spectrometer which encompasses the UV-visible and VUV ranges.

As plasma facilities become more complex and less accessible, the monitoring of line radiation with a monochromator is often inconvenient. Factors such as limited observation times and plasma irreproducibility suggest the use of multichannel systems. There are essentially two approaches currently in use to address these problems, viz multichannel adjacent detectors and a collection of detectors dedicated to particular wavelengths. The first method employs Micro Channel Plate (MCP) devices which can monitor the emitted spectrum in about 1000 adjacent channels [4-7]. While this approach is flexible in terms of wavelength choice and ideal for spectra survey applications it usually cannot simultaneously satisfy the conflicting requirements of wide wavelength range (eg Vac UV 500-2000Å or UV-Visible 3000Å-7000Å) and spectral resolution (typically 1Å to avoid significant line blending). The wavelength range encompassed by the MCP may be varied by altering the grating setting or selecting different gratings within a spectrometer [7] and thereby increasing the overall spectral coverage while at the same time preserving reasonable resolution. However, continuous monitoring of all the relevant wavelengths is sacrificed. The temporal response demanded depends on various factors such as impurity ionisation state evolution, plasma life time and detailed line intensity fluctuations. Generally, read out times of the MCP vary from ~ 1 msec for a few selected channels to ~ 15 msec for 1000 channels [6]. Although these effective time responses may be sufficient for long lived plasmas they are clearly inadequate for monitoring the evolution of impurities in our plasma device which has a typical 5 ms duration.

For short plasma discharge times, or observation of rapid fluctuations in the radiation intensity, a system with fast time response in a wide spectral range is required. A ten channel spectrometer has been reported elsewhere by Moreno and Marmar [8] which is similar to the one presented here but it lacks the capability for vacuum operation available to our instrument. The spectrometer described below was developed to monitor the time histories of emission lines in the VUV and the UV-visible regions (60-450 nm) for use as a general impurity diagnostic on the HBTX1A Reversed Field Pinch. To date only fibre optic coupling to the plasma has been possible which limits the present detectable wavelength range to ~ 220-450 nm.

INSTRUMENTAL

The Polychromator

The polychromator, a modified Rank Hilger model (E960 series), is capable of simultaneously observing time histories of up to 40 narrow band spectral regions. It is a single-chord instrument of Pacshen-Runge mount (Fig. 1) and incorporates a toroidal holographic grating (2442.4 lines/mm magnesium fluoride coated aluminium). This type of grating is attractive because it allows for relative high resolution; many emission lines of interest in high temperature plasmas may be separated by as little as 0.1 nm.

The grating is mounted at a medium incidence angle (≈ 35°), which is particularly useful due to its favourable reflectivity properties below 100 nm (eg [9]). Each of the pre-selected emission lines are observed by a detector, a side-windowed photomultiplier, which resides

in the spectrometer vacuum system. The input slit has the capability of fine movement along the Rowland circle via a micrometer spindle. The output slits are cut in a removable flexible foil which is also positioned at the Rowland circle. The grating mount and the slit system is supported in a three point ceramic kinematic mount for vibration and temperature isolation. Vacuum pressures of less than 10^{-7} Torr are obtainable with the present Viton 'O'- ring seals. However, with a differential pumping system (Fig. 1) and vacuum (gate) valves located along the flight tube (typical base pressure of 3×10^{-8} Torr), the polychromator may be used in direct access with the HBTX1A vacuum system which is at a nominal pressure of 10^{-8} Torr. The gate valves are normally closed but may be opened during the plasma discharge for minimal elevation of the torus base pressure.

The polychromator may be easily aligned with the torus viewing port by a He-Ne laser unit (Fig. 1). This unit is situated in the air side of the polychromator and uses the grating in the zero order mode.

To encompass a broad spectral region in the polychromator, the grating can be used in first and higher order modes along the same section of the Rowland circle (Table 1). A variety of light guides are used to direct the appropriate emission lines to photomultipliers: eg fibre-optics (quartz-'wet', Fibre Optiques Industries, France, fibre type QSF 200/300 ASW) in the longer wavelength range (> 220 nm) to suppress second or higher order wavelengths. The attenuation properties of the quartz fibre as shown in Fig. 2 may be taken as a guide [10]. Fibre-optics with a scintillator (eg. tetraphenyl-butadiene, [11]) are coated on the input face to observe shorter wavelengths. When higher order wavelengths are likely to

interfere (ie the interfering component is < 100 nm) aluminium mirrors (coated with magnesium fluoride used at small incidence angles) will be used to suppress the higher order shorter wavelengths. In this case the photomultiplier windows will be coated with a scintillator.

Occasional absolute calibration of the instrument can be obtained by the usual methods (eg Tungsten ribbon lamp for $\lambda \gtrsim 250$ nm, Deuterium lamp for $\lambda > 110$ nm or a synchrotron source for λ = 60-300 nm) but there is also the need for more routine calibrations which do not involve removing the instrument from the plasma machine. A pulsed UV xenon flashlamp source (Chelsea Instruments UK. model 3021) is initially cross calibrated and provides frequent absolute calibrations of the polychromator system. The deterioration of scintillator efficiency [11] and drifts in photomultiplier gains may be compensated for by the flashlamp source whose light intensity reproducibility is better than 1%.

The variation of inverse dispersion (the 'plate factor') along the Rowland circle, is given by:

$$d\lambda/d\ell = \frac{\cos\theta}{mRl}$$

m = diffraction order (1, 2 or 3 in our case)

R = Rowland circle diameter (750 mm)

l = rule density on grating; lines/mm (2442.4)

θ = the diffraction angle

ℓ = circumferential increment along the Rowland circle

The inverse dispersion along the image foil is approximately 0.5 nm/mm in the first order. Hence, with 1.2 mm wide input slits the spectral bands (or lines) of interest are selected so that the

separating wavelength interval to strong neighbouring lines is always greater than 0.6 nm.

The required impurity lines are located on the image foil using an equation of the form:

$$S(\lambda) = a[b-\mathrm{Sin}^{-1}(\lambda c-d)] - e$$

where $S(\lambda)$ is the position of the required slit with respect to the foil edge and here the constants a, b, c, d and e have been determined using appropriate spectral lamps.

The bandwidth characteristics of the polychromator system is dependent on the photomultiplier (80 MHz) and the amplifying systems which are electrically housed within the spectrometer manifold (Fig. 3) to reduce the electrical pick-up in the vicinity of the plasma machine. The amplified signals are recorded on a LSI-11 data acquisition system [12], which uses standard 1 MHz ADCs (Lecroy, quad 10 bit transient digitiser, model 8210). To avoid aliasing problems the amplifying systems (Fig. 3 inset) are given relatively low bandwidths (DC to 350 KHz, -3dB point) in contrast to the 80 MHz bandwidth capability of the photomultipliers. The amplifier channel separation is high and better than -120 dB (cf. the ADC channel separation better than -60 dB). The interfering component originates mostly from the amplifier power supply system. Noise was also negligible from the amplification system: 5 mV peak-peak (across 50 ohms) for the ADC signal window of 5V peak.

Wavelength Calibration

To date the polychromator has been used in the first order mode of the grating. The input to the polychromator consists of a quartz fibre-optic which is coupled to a port on HBTX1A (Fig 1, inset). Note

that, due to the attenuation properties of the quartz fibre optics (cf Fig. 2), second order wavelengths will be suppressed (for $\lambda \lesssim 220$ nm).

An input slit is precision-cut onto a thin rigid rectangular metal foil which rests upon reference edges along the Rowland circle. With the output foil containing the impurity-line set (Table 2), wavelength calibration (mercury lamp) is achieved by cutting two reference slits (these slits are narrow (100 μm) compared with the impurity line slits of 1.2 mm). For a wavelength calibration an input slit of the same dimensions as the reference slits is used.

The variation of photomultiplier output corresponding to the 365.0 nm emission line, as the input slit is translated, is shown in Fig. 4a. The photomultiplier also sees the smaller peaks corresponding to weak neighbouring mercury lines 365.5 and 366.33 nm. In practice, we may encounter overlap problems as these neighbouring images are wider for larger input slits. Since the micrometer spindle reading is an indication of the input slit position the peak separation is closer by a factor of $\mathrm{Cos}\phi/\mathrm{Cos}\theta$. This factor is due to the variation of inverse dispersion along the Rowland circle.

An instrumental width (FWHM) of $\sim$ 0.067 nm was measured for 100 μm input/output slits. We can observe the irregular fall-off in intensity at the spectral edges (eg Fig. 4b), due mostly to off-axis components originating from the irregular edges of the straight input slit. For the 253.65 nm line (Fig. 4b) we see that the peak has shifted on the micrometer scale. This is due to the positional inaccuracy ($\approx$ 0.15 mm) during the cutting process, which uses the spark erosion technique.

New foils will be cut using high accuracy laser (~ 15 μm) cutting techniques.

The impurity emission lines are chosen to avoid strong interfering adjacent wavelengths (a spectral 'neighbour' in the image plane). Generally, strong transitions, preferably resonant, are chosen wherever possible so that the interfering component intensity (if present) is relatively small. For the initial operation of the polychromator, with the non-resonant emission lines shown in Table 2, the optimum input and output slit widths were set at 1.2 mm.

COMMISSIONING AND INITIAL RESULTS

The polychromator was installed on the HBTX1A [1] Reversed Field Pinch experiment to monitor the behaviour of low ionisation state impurities. Plasma discharges with standard conditions [13] (2 mTorr fill pressure, 200 kA peak current, self reversal and with power crowbar) are used in this study. Typical parameters of the HBTX1A plasma are electron density $n_e \sim 10^{13} cm^{-3}$, electron temperature T_e = 100-350 eV, ion temperature $T_i \geq T_e$, ratio of radiated power to ohmic input power [16] $P_{rad}/P_{ohmic} \sim 3\%$; main impurity concentrations:- Carbon (2%), Oxygen (1%) and Iron (0.1%).

The spectrometer views a central chord through the plasma and also sees the inside wall of the vacuum vessel. Typical raw data from the polychromator are shown in Fig. 5. Most observations are obtained in parallel with a visible monochromator (Rank Hilger 'Monospek' 1000:range 200-1000 nm), which can observe the same plasma chord as the polychromator (via another quartz fibre), or can view an alternative plasma chord (toroidally displaced by 22 degrees from the polychromator port) which views a light dump. The monochromator which was previously

checked to have little stray light, is used as a 'standard' to compare with the polychromator output. (The monochromator had stray light intensities which are negligible compared with the spectral line intensities. For example, when the instrument setting is changed from the D_α line (656.1 nm) to a region free of spectral lines at 632.8 nm the signal decreased by about 3 orders of magnitude.) Using digital comparison techniques, time histories of the impurity line intensities from the polychromator are compared with the monochromator signals (viewing the same plasma chord as the polychromator). It was concluded that the stray light in the polychromator is comparable to that in the monochromator.

All but one of the emission lines chosen during commissioning of the instrument are free from strong interfering lines which allowed for monitoring of the corresponding ion state behaviour. However, a weak overlapping emission line on the CIV channel is observed. A spectral survey [14] showed that the intefering line is from FeI (252.3 nm). In Fig. 6a and 6b, digitally filtered traces (low pass filter, 31 kHz, -3db point) show the time histories of the CIV and FeII channel outputs respectively. The FeII radiation peaks during certain times of the plasma discharge which is mirrored, to a lesser extent, in the CIV channel.

Since the polychromator is a single chord instrument, it is possible (if the interfering impurity ion state is observed on another transition) to digitally 'subtract' the interfering line.

We may regard the time histories of FeI and FeII to be very similar. This is due to the fact that low-ionization Iron radiation mainly originates from the plasma periphery due to the large

concentrations of iron (the liner) and the small amounts of energy needed to ionise FeI to FeII [2] and FeII to FeIII.

To first order, we may obtain the true CIV time history, by using the fact that the emission fluctuations of the CIV channel cross correlates with FeII signal better than CV or CIII does with FeII. We may therefore interpolate to the spectrally 'pure' CIV due to its relative spatial overlap in the plasma with the CIII and CV distributions, so that correlation between CIV and FeII lies between that of CV (with FeII) and CIII (with FeII). Ideally, if the behaviour of the interfering impurity, as represented by the spectral line intensity, were completed decoupled from the behaviour of the CIV ion state it would be relatively straightforward to remove its effect. For example, we might cross correlate the difference signal I (CIV) - α I (FeII) with I (FeII) where I (CIV) and I (FeII) are the signals from the CIV and FeII channels, respectively and α is a multiplication factor which is varied until minimum correlation is obtained. The true CIV signal would then be given by I (CIV) - α_{mm} I (FeII). However, the behaviour of the different impurity species and ions, or at least the line intensities, are not independent of each other as can be seen from a comparison of Fig 6b (FeII) with Fig 6c (CIII) and Fig 6d (CV). Because of the spatial distribution of the CIII, CIV and CV ion states in the plasma we would expect the correlation of the true CIV signal with FeII to be intermediate between that of CIII and CV. Assuming that the location of the ion states in the plasma is a significant factor in determining the correlation with the FeII radiation, at the periphery, we calculate the spatial distribution of the CIII, CIV and CV states and using this information we obtained experimental cross

correlation coefficients [15] with FeII, first as a function of ion state and then as a function of space. This exercise enables us to obtain an estimate of the expected correlation coefficient for CIV with FeII. The value of α is varied until the experimental determination of the correlation coefficient from the CIV and FeII channels agrees with the expected one. The resultant CIV time history obtained by this method is shown in Fig. 6e. The main point we wish to draw attention to is that intefering lines may in some cases be removed due to the single chord nature of the polychromator and its relatively wide bandwidth. Obviously, it is preferable to avoid intefering lines from the outset but this may not always be possible because, for example, of the presence of unexpected impurities or limited wavelength range in the instrument.

The wide bandwidth of the polychromator system has many advantages where, for example, fluctuation and correlation studies may be performed using fast fourier transform techniques. Low pass digital gaussian filters may also be used to study low frequency phenomena, eg burn through of Oxygen and Carbon (10 KHz filter: Fig. 7a, b) which may be used to determine the impurity influx and transport rates.

Summary

The polychromator described here is a multichannel spectrometer that provides simultaneous observation of selected emission bands and lines in the 220-450 nm spectral range with good frequency response (350 kHz). The instrument may also be used to derive the time history of a blended emission line by 'subtracting' the interfering line, if the same, or similar, ionisation state is separately observed. Although the instrument is at present used in the first order range, it

will in future include higher grating orders by using the spectrometer in vacuum mode, and so increase the spectral range to cover 60-450 nm.

ACKNOWLEDGEMENTS

The authors would like to thank T Dodd, R K Hall and A R Field for their help in the development of the polychromator. We are also indebted to Drs M Malacarne and D Brotherton-Ratcliffe for useful discussions involving fast-fourier transformer analyses.

References

[1] H A B Bodin and A A Newton, Nuclear Fusion 20, 1255 (1980).

[2] P G Carolan and V A Piotrowicz, Plasma Physics 25, 1065 (1983)

[3] G M McCracken and P E Stott, Nuclear Fusion 19, 889 (1979)

[4] W L Hodge,, B C Stratton and H W Moos, Rev. Sci. Instrum. 55, 16 (1984).

[5] R J Fonck, A T Ramsey and R V Yelle, Appl. Opt., 12, 2115, (1982).

[6] N C Hawkes and N J Peacock, Nucl. Fusion to be published

[7] R E Bell, M Finkenthal and H W Moos, Rev. Sci. Instrum. 52, 1806 (1981)

[8] J C Moreno and E S Marmar, Phys. Rev. A 31, 3291 (1985)

[9] 'Physics of Thin Films', Academic Press, 10 (1978)

[10] A R Field and W Thompson, Culham Laboratory private communication (1985). Culham Laboratory Report in preparation CLMR259 1985

[11] W M Burton and B A Powell, App. Opt., 12, 87 (1973).

[12] G S Cross, K Fullard, A H Reed and K Reed, Proc. of the 11th Symposium of Fusion Technology 1, 477, (1978).

[13] P G Carolan et al, Plasma Phys. and Contr. Nucl. Fusion Res. 1984 (Proc. 10th Conf London) 2, 449, IAEA Vienna (1985).

[14] P G Carolan, A M Manley, N C Hawkes and N J Peacock, Culham Laboratory Report CLM R260 (1985)

[15] 'Principles and Applications of Random Noise Theory' by J S Bendat, J Wiley and Sons (1958).

[16] C A Bunting, P G Carolan, D G Muir, 11th European Conference on Controlled Fusion and Plasma Physics, Aachen, part 1, p155, (1983).

Table 1

Wavelength range of the polychromator for the grating order 1-3 and the appropriate guidance employed for routing the light to the photomultipliers.

Grating Order m	Wavelength Range (nm)	Light Guidance
1	175-450	fibre-optic bundles (>220 nm) Al mirrors (λ>110 nm)
2	87-220	Al mirrors (110 nm < λ < 220 nm), scintillator coated fibre-topic bundle (λ < 220 nm)
3	≈60-220	scintillator coated fibre-optic bundle

Table 2

Present selection of impurity lines used. The grating is operated in first order only and the polychromator has a quartz fibre input which limits the lower wavelength detection to about 220 nm.

Ion State	Transition	Wavelength (nm)	Ionization Potential (eV)
CII	3d - 4f	426.720	24.3
CIII	$2s2p - 2p^2$	229.790	47.9
CIV	4d - 5f	252.440	64.5
CV	2s - 2p	227.090	392.1
OII	3s - 3p	441.491	35.1
OIII	3p - 3d	326.098	54.9
OIV	3s - 3p	338.128	77.4
OV	3s - 3p	278.090	113.9
FeII		259.837	16.2
HgI		253.6 (wavelength calibration lines)	
HgI		365.0	

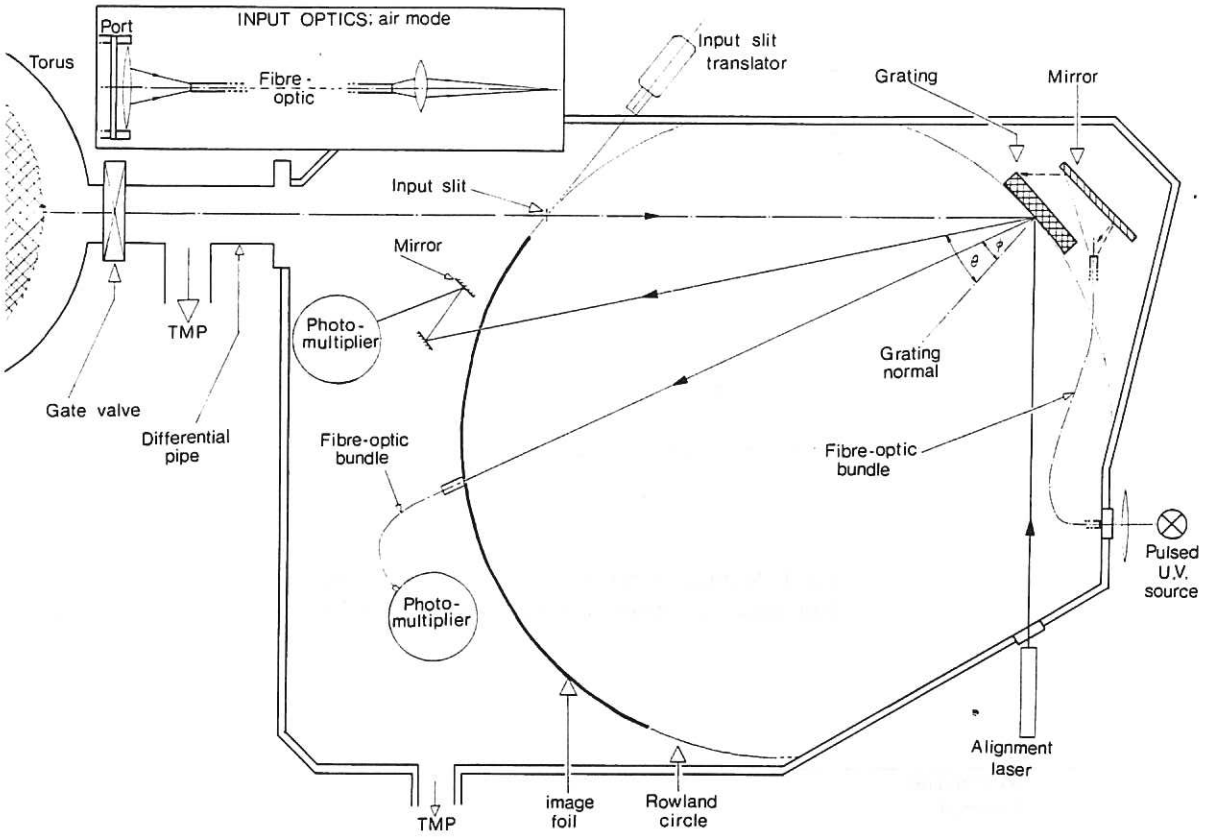

Fig. 1 The polychromator layout (only two output channels shown).

CLM-P753

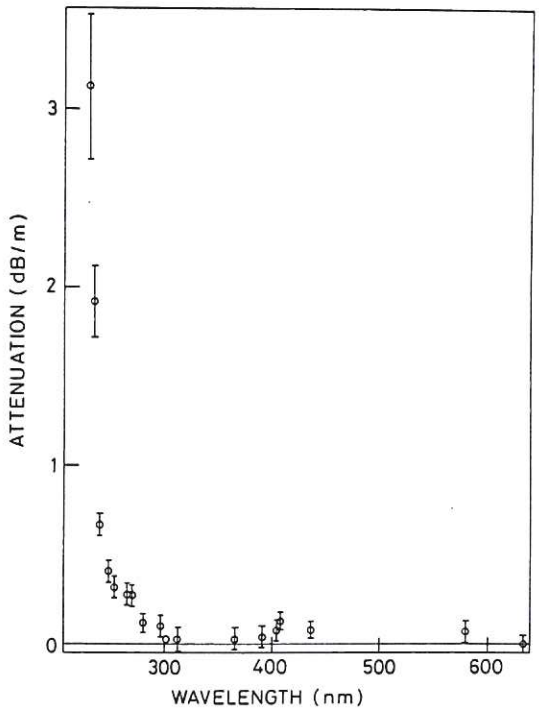

Fig. 2 Attenuation of quartz ('wet') fibre—(Fibre Optiques Industries, France, type QSF600W).

CLM-P753

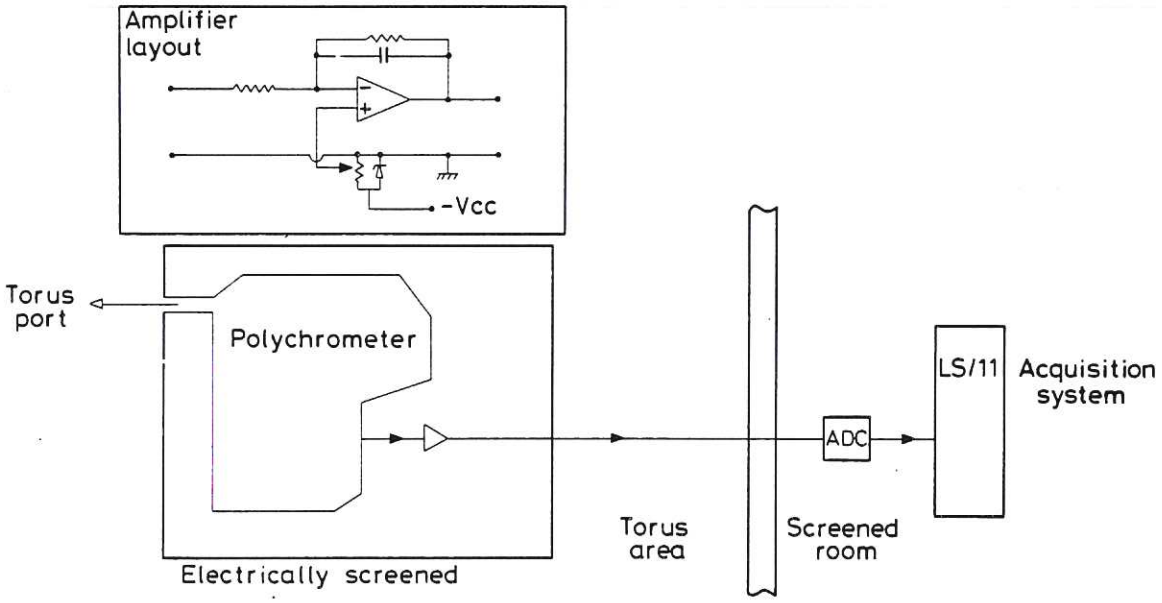

Fig. 3 Electrical layout of the polychromator and data acquisition systems.

CLM-P753

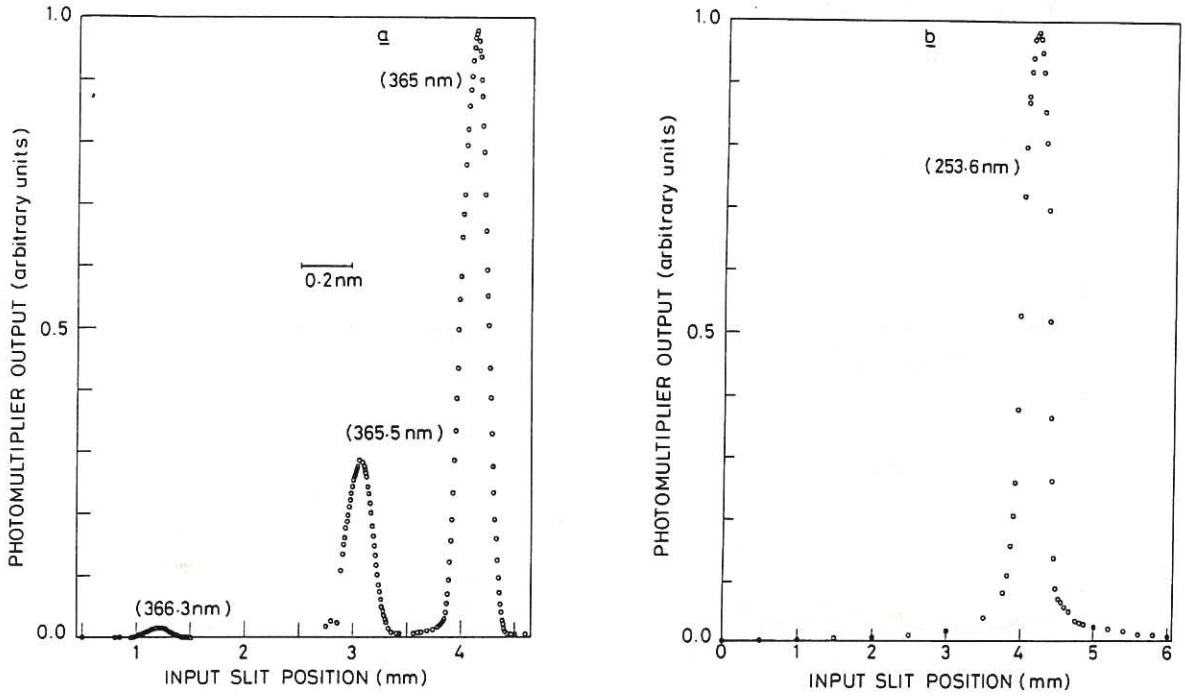

Fig. 4 Photomultiplier response with input slit transition with a mercury lamp on (a) the 365 nm channel and (b) 253.6 nm channel.

CLM-P753

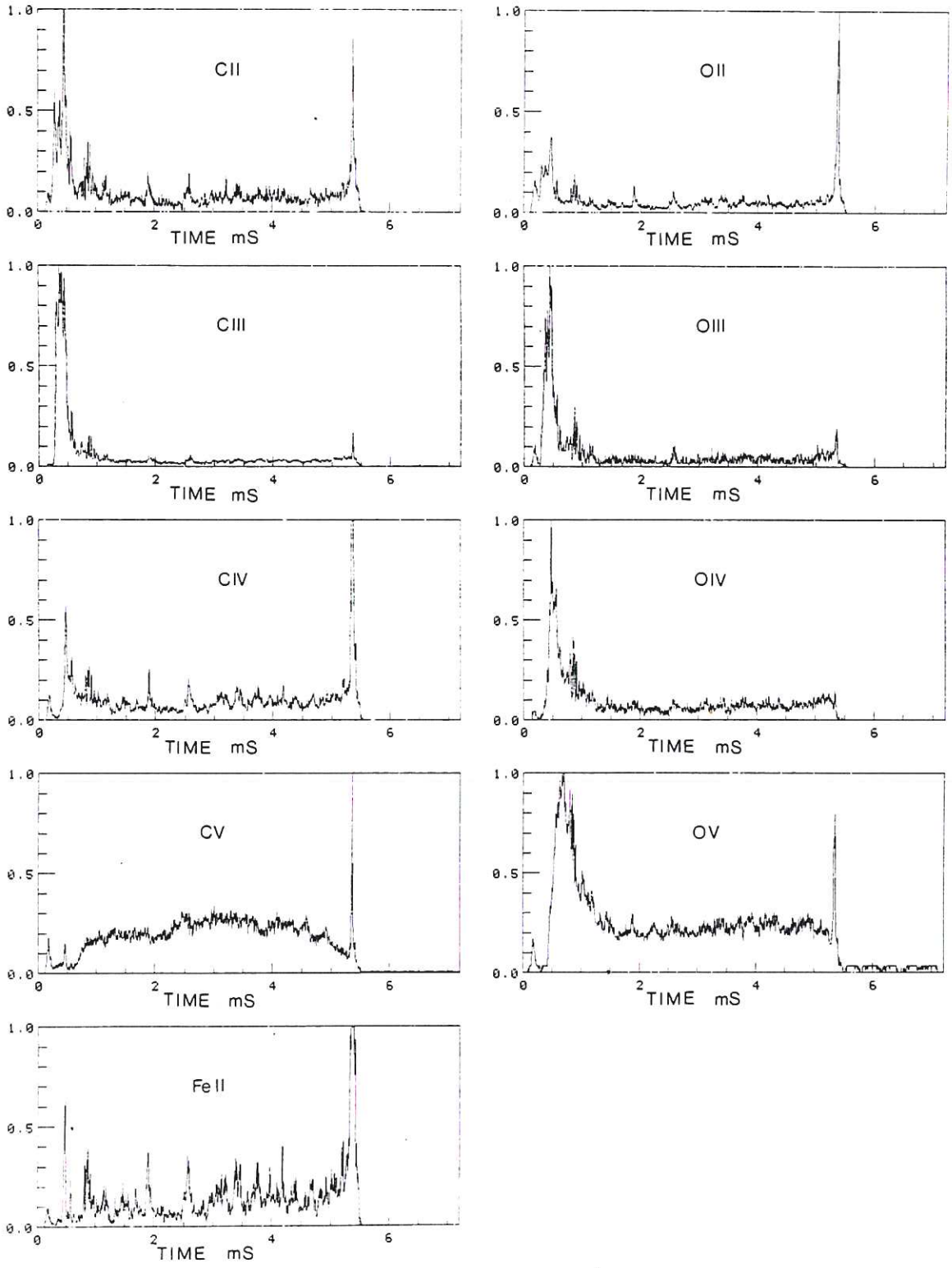

Fig. 5 Raw signals from the polychromator.

CLM-P753

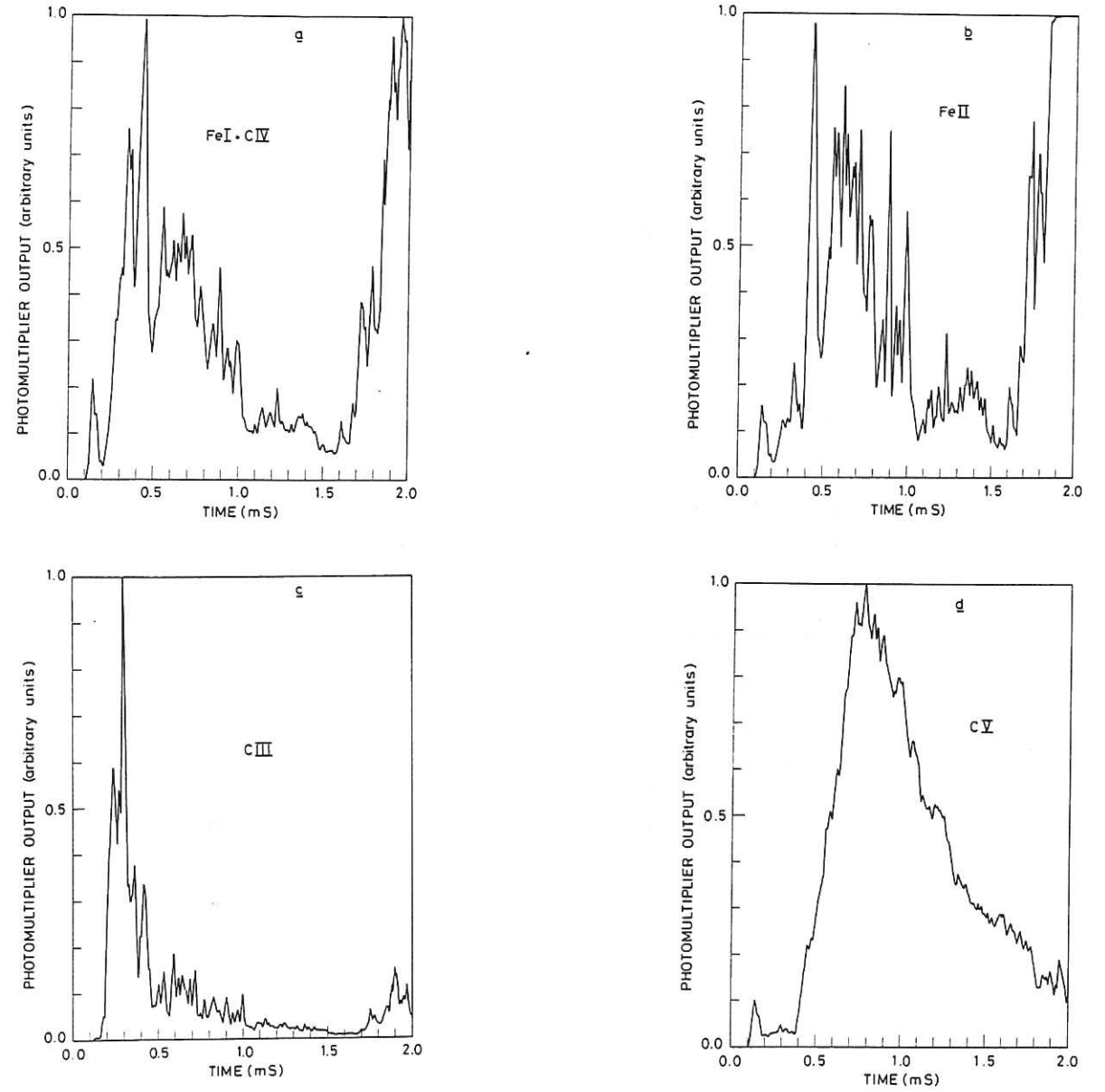

Fig. 6 Time history of (a) interfered CIV channel, (b) FeII channel, (c) CIII channel, (d) CV channel and (e) the corrected CIV output.

CLM-P753

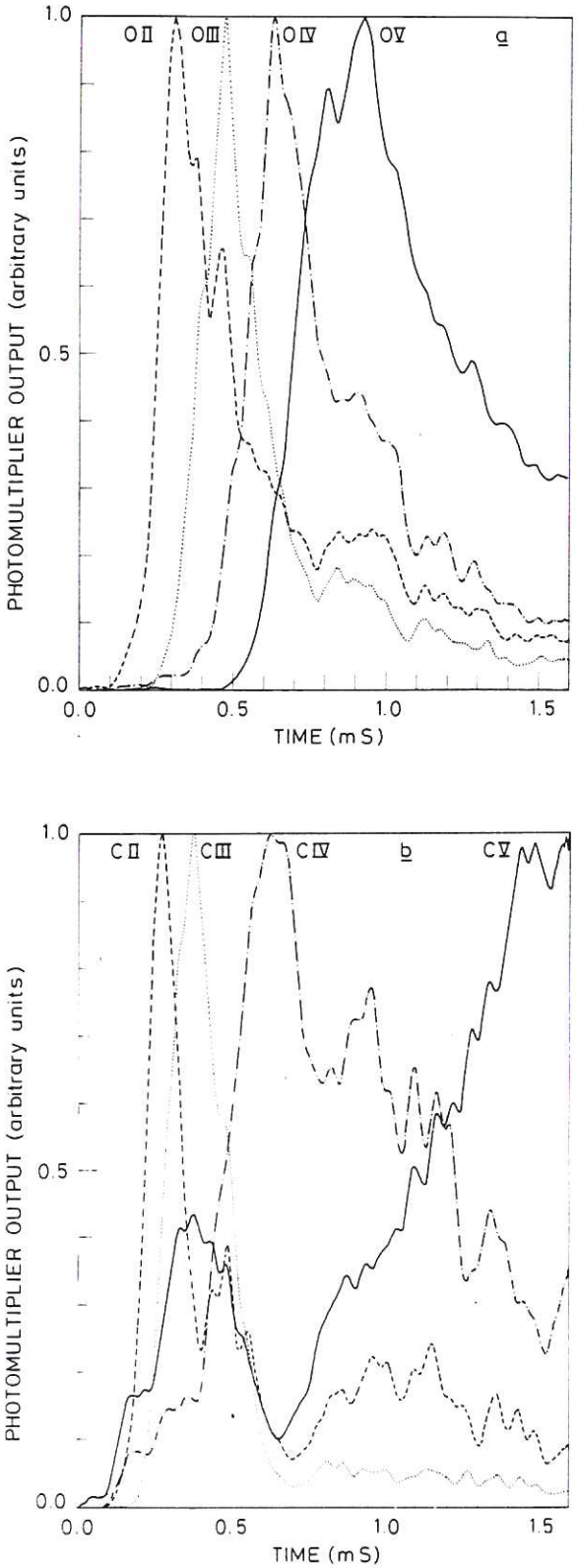

Fig. 7 Burn through of (a) Oxygen and (b) Carbon.

CLM-P753